

Isospin corrections for superallowed Fermi β decay in self-consistent relativistic random-phase approximation approaches

Haozhao Liang (梁豪兆),^{1,2} Nguyen Van Giai,² and Jie Meng (孟杰)^{1,3}

¹State Key Laboratory of Nuclear Physics and Technology, School of Physics, Peking University, Beijing 100871, People's Republic of China

²Institut de Physique Nucléaire, IN2P3-CNRS and Université Paris-Sud, F-91406 Orsay Cedex, France

³Department of Physics, University of Stellenbosch, Stellenbosch, South Africa

(Received 23 April 2009; published 18 June 2009)

Self-consistent random phase approximation (RPA) approaches in the relativistic framework are applied to calculate the isospin symmetry-breaking corrections δ_c for the $0^+ \rightarrow 0^+$ superallowed transitions. It is found that the corrections δ_c are sensitive to the proper treatments of the Coulomb mean field, but not so much to specific effective interactions. With these corrections δ_c , the nucleus-independent $\mathcal{F}t$ values are obtained in combination with the experimental ft values in the most recent survey and the improved radiative corrections. It is found that the constancy of the $\mathcal{F}t$ values is satisfied for all effective interactions employed. Furthermore, the element V_{ud} and unitarity of the Cabibbo-Kobayashi-Maskawa matrix are discussed.

DOI: 10.1103/PhysRevC.79.064316

PACS number(s): 23.40.Bw, 12.15.Hh, 21.60.Jz, 24.10.Jv

I. INTRODUCTION

The Cabibbo-Kobayashi-Maskawa (CKM) matrix [1,2] relates the quark eigenstates of the weak interaction with the quark mass eigenstates. The unitarity condition of the CKM matrix provides a rigorous test for the standard model description of electroweak interactions. Its leading matrix element, V_{ud} , only depends on the first generation quarks and so is the element that can be determined most precisely. There are three traditional methods to determine $|V_{ud}|$ experimentally: nuclear $0^+ \rightarrow 0^+$ superallowed Fermi β decays [3], neutron decay [4], and pion β decay [5]. Recently, experiments with nuclear mirror transitions provided another independent sensitive source for extracting the value of $|V_{ud}|$ [6].

Among these methods, the most precise determination of $|V_{ud}|$ comes from the study of nuclear $0^+ \rightarrow 0^+$ superallowed Fermi β decays [7]. These pure Fermi transitions between nuclear isobaric analog states (IAS) allow for a direct measurement of the vector coupling constant G_V of semileptonic weak interactions by

$$G_V^2 = \frac{K}{2(1 + \Delta_R^V)\mathcal{F}t}. \quad (1)$$

Together with the Fermi coupling constant G_F for purely leptonic decays, the up-down element of the CKM matrix can be determined, $V_{ud} = G_V/G_F$. In Eq. (1), $K/(\hbar c)^6 = 2\pi^3\hbar \ln 2/(m_e c^2)^5$ and Δ_R^V is the transition-independent part of radiative corrections caused, for example, by the processes where the emitted electron may emit a bremsstrahlung photon that goes undetected in the experiment [8,9]. The nucleus-independent $\mathcal{F}t$ value is obtained by the corrections to the experimental ft values for radiative effects as well as isospin symmetry breaking by Coulomb and charge-dependent nuclear forces [3],

$$\mathcal{F}t = ft(1 + \delta'_R)(1 + \delta_{NS} - \delta_c), \quad (2)$$

where f and t represent the statistical rate function and partial half-life, respectively, and are obtained through measurements of the Q values, branching ratios, and half-lives

for the superallowed decays. The correction terms δ'_R and δ_{NS} represent the transition-dependent radiative corrections [8,9]. The correction term δ_c is the isospin symmetry-breaking correction, accounting for the isospin symmetry breaking in nuclei.

The isospin is not an exact symmetry mainly due to the presence of the Coulomb forces in nuclei. The nonconservation of isospin symmetry induces a slight reduction of the superallowed transition strength $|M_F|^2$ from its ideal value $|M_0|^2$:

$$|M_F|^2 = |\langle f|T_{\pm}|i\rangle|^2 = |M_0|^2(1 - \delta_c), \quad (3)$$

where $M_0 = \sqrt{2}$ for $T = 1$ states with the exact isospin symmetry.

Shell model calculations are generally used to determine the isospin symmetry-breaking corrections δ_c . Recently, by including the core orbitals, an improvement on such corrections has been achieved and a good agreement among the nucleus-independent $\mathcal{F}t$ values for the 13 well-measured cases has been obtained [9].

Alternatively, the self-consistent random phase approximation (RPA) based on microscopic mean field theories is another reliable approach for the superallowed transition strength M_F . Such calculations were performed for a few nuclei with the nonrelativistic Skyrme Hartree-Fock approach in the 1990s [10]. Since then no further investigation followed even though significant progress in self-consistent RPA in charge-exchange channels have been made [11–15].

During the last decade, great efforts have been dedicated to developing the charge-exchange (Q)RPA within the relativistic framework. From the early model which only contains a rather small configuration space [13] to the sophisticated model which includes Bogoliubov transformation and proton-neutron pairing [14], these approaches are aimed at describing the spin-isospin resonances, β decay rates, neutrino-nucleus cross sections, etc., in a systematical, reliable, and predictive way. Recently, based on the success of the newly established density-dependent relativistic Hartree-Fock (RHF) approach [16–18], a fully self-consistent charge-exchange RPA has been

established and the first applications have been performed for spin-isospin resonances like Gamow-Teller and spin-dipole resonances [15]. A very satisfactory agreement with the experimental data was obtained without any readjustment of the energy functional. Therefore, it is appropriate now to reinvestigate the isospin corrections for superallowed Fermi β decay with these relativistic approaches. It is not the aim here to claim that a covariant framework is necessarily more appropriate for this problem than a nonrelativistic one such as Skyrme Hartree-Fock plus RPA. The key point, which will be discussed in Sec. III A, is a full treatment of Coulomb and nuclear interactions in both their direct and exchange contributions. In this respect, satisfactory nonrelativistic RPA studies of the δ_c corrections are not available.

In this paper, the self-consistent RPA approaches in the relativistic framework will be applied to calculate the isospin symmetry-breaking corrections δ_c . With the corrections thus obtained, the nucleus-independent $\mathcal{F}t$ values will be obtained in combination with the experimental ft values in the most recent survey [19] and the improved radiative corrections [8,9]. The element V_{ud} and unitarity of the CKM matrix will then be discussed.

II. SELF-CONSISTENT RELATIVISTIC RPA

The basic ansatz of the relativistic Hartree (RH), also known as relativistic mean field (RMF), and relativistic Hartree-Fock (RHF) theories is a Lagrangian density \mathcal{L} , where nucleons are described as Dirac spinors that interact via the exchange of σ -, ω -, ρ -, π -mesons and the photon [20–22]. In order to give a satisfactory description of nuclear matter and finite nuclei, the nonlinear self-coupling of mesons, e.g., in Refs. [23–25], or density-dependent meson-nucleon couplings, e.g., in Refs. [16,26], are introduced.

The effective Hamiltonian operator \hat{H} can be obtained with the general Legendre transformation. Together with the trial ground state (Slater determinant) in the Hartree or Hartree-Fock approximation, the energy functional can be written as

$$\begin{aligned} E &= \langle \Phi_0 | \hat{H} | \Phi_0 \rangle \\ &= \sum_a \langle a | \alpha \cdot \mathbf{p} + \beta M | a \rangle + \frac{1}{2} \sum_{ab} \langle ab | V(1, 2) | ba \rangle \\ &\quad - \frac{1}{2} \sum_{ab} \langle ab | V(1, 2) | ab \rangle, \end{aligned} \quad (4)$$

where the first term is the kinetic energy, the second and the last terms are the direct (Hartree) and exchange (Fock) energies, respectively. In the Hartree approximation, the Fock term is neglected for simplicity. The two-body interaction $V(1, 2)$ includes the following meson-nucleon and photon-nucleon interactions:

$$V_\sigma(1, 2) = -[g_\sigma \gamma_0]_1 [g_\sigma \gamma_0]_2 D_\sigma(1, 2), \quad (5a)$$

$$V_\omega(1, 2) = [g_\omega \gamma_0 \gamma^\mu]_1 [g_\omega \gamma_0 \gamma_\mu]_2 D_\omega(1, 2), \quad (5b)$$

$$V_\rho(1, 2) = [g_\rho \gamma_0 \gamma^\mu \vec{\tau}]_1 \cdot [g_\rho \gamma_0 \gamma_\mu \vec{\tau}]_2 D_\rho(1, 2), \quad (5c)$$

$$V_\pi(1, 2) = - \left[\frac{f_\pi}{m_\pi} \vec{\tau} \gamma_0 \gamma_5 \gamma^k \partial_k \right]_1 \cdot \left[\frac{f_\pi}{m_\pi} \vec{\tau} \gamma_0 \gamma_5 \gamma^l \partial_l \right]_2 D_\pi(1, 2), \quad (5d)$$

$$V_A(1, 2) = \frac{e^2}{4} [\gamma_0 \gamma^\mu (1 - \tau_3)]_1 [\gamma_0 \gamma_\mu (1 - \tau_3)]_2 D_A(1, 2), \quad (5e)$$

with the finite-range Yukawa type propagator

$$D_i(1, 2) = \frac{1}{4\pi} \frac{e^{-m_i |\mathbf{r}_1 - \mathbf{r}_2|}}{|\mathbf{r}_1 - \mathbf{r}_2|}. \quad (6)$$

Furthermore, in order to cancel the contact interaction coming from the pion pseudovector coupling, a zero-range pionic counterterm should be included [15,21]:

$$V_{\pi\delta}(1, 2) = g' \left[\frac{f_\pi}{m_\pi} \vec{\tau} \gamma_0 \gamma_5 \boldsymbol{\gamma} \right]_1 \cdot \left[\frac{f_\pi}{m_\pi} \vec{\tau} \gamma_0 \gamma_5 \boldsymbol{\gamma} \right]_2 \delta(\mathbf{r}_1 - \mathbf{r}_2), \quad (7)$$

with $g' = 1/3$. Thus, g' is not an adjustable parameter.

The RPA equations can be obtained by taking the second derivative of the energy functional E . In the charge-exchange channels, the RPA equations become

$$\begin{pmatrix} \mathcal{A}_{p\bar{n}p'\bar{n}'}^J & \mathcal{B}_{p\bar{n}n'\bar{p}'}^J \\ -\mathcal{B}_{n\bar{p}p'\bar{n}'}^J & -\mathcal{A}_{n\bar{p}n'\bar{p}'}^J \end{pmatrix} \begin{pmatrix} U_{p'\bar{n}'}^{J\nu} \\ V_{n'\bar{p}'}^{J\nu} \end{pmatrix} = \omega_\nu \begin{pmatrix} U_{p\bar{n}}^{J\nu} \\ V_{n\bar{p}}^{J\nu} \end{pmatrix}, \quad (8)$$

where p and \bar{p} (n and \bar{n}) denote unoccupied and occupied proton (neutron) states. These equations describe both the T_+ and T_- channels. It should be emphasized that the unoccupied states include not only the states above the Fermi surface, but also the states in the Dirac sea. The RPA matrices \mathcal{A} and \mathcal{B} read

$$\mathcal{A}_{12,34} = (E_1 - E_2) \delta_{12,34} + \langle 14 | V_{\text{ph}} | 32 - 23 \rangle, \quad (9a)$$

$$\mathcal{B}_{12,34} = - \langle 13 | V_{\text{ph}} | 42 - 24 \rangle, \quad (9b)$$

where the first term in the ket represents the direct contribution, and the second term represents the exchange contribution. In the RPA built on the Hartree mean field, the exchange contributions in Eqs. (9) are accordingly neglected.

In the self-consistent RPA calculations, the particle-hole residual interaction V_{ph} should be derived from the same energy functional E as that used in the ground-state description. The explicit density dependence of the meson-nucleon couplings introduces, in principle, additional rearrangement terms in the particle-hole residual interaction V_{ph} , and their contributions are essential for a quantitative description of excited states [27]. However, since the rearrangement terms are due to the dependence on isoscalar ground-state densities, it is easy to see that they are absent in the charge-exchange channels. Therefore, in the description of superallowed Fermi β decays, the particle-hole residual interaction V_{ph} is just the meson-nucleon interactions shown in Eqs. (5a)–(5d) and (7). The photon-nucleon interaction in Eq. (5e) does not contribute to the particle-hole residual interaction because the configurations are of the neutron-proton type.

The eigenvectors of the RPA equations (8) are separated into two groups, which respectively represent the excitations of the T_- and T_+ channels with the following normalization conditions:

$$\begin{cases} \sum_{p\bar{n}} (U_{p\bar{n}}^{J\nu})^2 - \sum_{n\bar{p}} (V_{n\bar{p}}^{J\nu})^2 = +1, & \text{for } T_- \text{ channel,} \\ \sum_{p\bar{n}} (U_{p\bar{n}}^{J\nu})^2 - \sum_{n\bar{p}} (V_{n\bar{p}}^{J\nu})^2 = -1, & \text{for } T_+ \text{ channel.} \end{cases} \quad (10)$$

Then, the excitation energies and X, Y amplitudes in the T_- channel read

$$\Omega_\nu = +\omega_\nu, \quad X_{p\bar{n}}^{J\nu} = U_{p\bar{n}}^{J\nu}, \quad Y_{n\bar{p}}^{J\nu} = V_{n\bar{p}}^{J\nu}, \quad (11)$$

whereas the excitation energies and X, Y amplitudes in the T_+ channel are

$$\Omega_\nu = -\omega_\nu, \quad X_{n\bar{p}}^{J\nu} = V_{n\bar{p}}^{J\nu}, \quad Y_{p\bar{n}}^{J\nu} = U_{p\bar{n}}^{J\nu}. \quad (12)$$

The $0^+ \rightarrow 0^+$ superallowed transition operators are T_- or T_+ . The transition probabilities between the ground-state and excited states read

$$B_{J\nu}^- = \left| \sum_{p\bar{n}} X_{p\bar{n}}^{J\nu} \langle p || T_- || \bar{n} \rangle + \sum_{n\bar{p}} (-)^{j_n+j_{\bar{p}}} Y_{n\bar{p}}^{J\nu} \langle \bar{p} || T_- || n \rangle \right|^2, \quad (13a)$$

$$B_{J\nu}^+ = \left| \sum_{n\bar{p}} X_{n\bar{p}}^{J\nu} \langle n || T_+ || \bar{p} \rangle + \sum_{p\bar{n}} (-)^{j_p+j_{\bar{n}}} Y_{p\bar{n}}^{J\nu} \langle \bar{n} || T_+ || p \rangle \right|^2. \quad (13b)$$

Before ending this section, it is worthwhile to make the following remark about the self-consistency of the RH+RPA approach when it is applied to the $0^+ \rightarrow 0^+$ transitions. Within this approach, it is known that, in order to reproduce the

excitation energies of Gamow-Teller resonances, one has to adjust the πNN particle-hole residual interaction and that g' cannot be kept equal to 1/3 [13,14]. However, for the $0^+ \rightarrow 0^+$ channel in the present paper, the direct contributions from the pion vanish. Therefore, in this sense, the self-consistency is also fulfilled in RH+RPA approach for the superallowed Fermi β decays.

III. RESULTS AND DISCUSSION

For all the calculations in this paper, the spherical symmetry is assumed and the filling approximation is applied to the last partially occupied orbital. The radial Dirac equations are solved in coordinate space by the Runge-Kutta method within a spherical box with a box radius $R = 15$ fm and a mesh size $dr = 0.1$ fm [28]. The single-particle wave functions thus obtained are used to construct the RPA matrices \mathcal{A} and \mathcal{B} in Eqs. (9) with the single-particle energy truncation $[-M, M + 120$ MeV], i.e., the occupied states are the positive energy states below the Fermi surface, whereas the unoccupied states can be either positive energy states above the Fermi surface or bound negative energy states [15]. With these numerical inputs, the model-independent sum rule,

$$\sum_\nu B_\nu^- - \sum_\nu B_\nu^+ = N - Z, \quad (14)$$

can be fulfilled up to 10^{-5} accuracy, and the isospin symmetry-breaking corrections δ_c are stable with respect to these numerical inputs at the same level of accuracy.

A. Isospin symmetry-breaking correction δ_c

In Table I, the isospin symmetry-breaking corrections δ_c in Eq. (3) for the $0^+ \rightarrow 0^+$ superallowed transitions are shown. The results are obtained by self-consistent RHF+RPA

TABLE I. Isospin symmetry-breaking corrections δ_c for the $0^+ \rightarrow 0^+$ superallowed transitions obtained by self-consistent RHF+RPA calculations with PKO1 [16], PKO2 [29], and PKO3 [29] as well as self-consistent RH+RPA calculations with DD-ME1 [26], DD-ME2 [30], NL3 [23], and TM1 [24]. The column PKO1* presents the results obtained with PKO1 without the Coulomb exchange (Fock) term. The results obtained by shell model calculations [9] are listed in the column T&H for comparison. All values are expressed in percents.

	PKO1	PKO2	PKO3	PKO1*	DD-ME1	DD-ME2	NL3	TM1	T&H [9]
$^{10}\text{C} \rightarrow ^{10}\text{B}$	0.082	0.083	0.088	0.148	0.149	0.150	0.124	0.133	0.175(18)
$^{14}\text{O} \rightarrow ^{14}\text{N}$	0.114	0.134	0.110	0.178	0.189	0.197	0.181	0.159	0.330(25)
$^{18}\text{Ne} \rightarrow ^{18}\text{F}$	0.270	0.277	0.288	0.357	0.424	0.430	0.344	0.373	0.565(39)
$^{26}\text{Si} \rightarrow ^{26}\text{Al}$	0.176	0.176	0.184	0.246	0.252	0.252	0.213	0.226	0.435(27)
$^{30}\text{S} \rightarrow ^{30}\text{P}$	0.497	0.550	0.507	0.625	0.612	0.633	0.551	0.648	0.855(28)
$^{34}\text{Ar} \rightarrow ^{34}\text{Cl}$	0.268	0.281	0.267	0.359	0.368	0.376	0.438	0.320	0.665(56)
$^{38}\text{Ca} \rightarrow ^{38}\text{K}$	0.313	0.330	0.313	0.406	0.431	0.441	0.390	0.572	0.765(71)
$^{42}\text{Ti} \rightarrow ^{42}\text{Sc}$	0.384	0.387	0.390	0.460	0.515	0.523	0.436	0.443	0.935(78)
$^{26}\text{Al} \rightarrow ^{26}\text{Mg}$	0.139	0.138	0.144	0.193	0.198	0.198	0.172	0.179	0.310(18)
$^{34}\text{Cl} \rightarrow ^{34}\text{S}$	0.234	0.242	0.231	0.298	0.302	0.307	0.289	0.267	0.650(46)
$^{38}\text{K} \rightarrow ^{38}\text{Ar}$	0.278	0.290	0.276	0.344	0.363	0.371	0.334	0.484	0.655(59)
$^{42}\text{Sc} \rightarrow ^{42}\text{Ca}$	0.333	0.334	0.336	0.395	0.442	0.448	0.377	0.383	0.665(56)
$^{54}\text{Co} \rightarrow ^{54}\text{Fe}$	0.319	0.317	0.321	0.392	0.395	0.393	0.355	0.368	0.770(67)
$^{66}\text{As} \rightarrow ^{66}\text{Ge}$	0.475	0.475	0.469	0.571	0.568	0.572	0.560	0.524	1.56(40)
$^{70}\text{Br} \rightarrow ^{70}\text{Se}$	1.140	1.118	1.107	1.234	1.232	1.268	1.230	1.226	1.60(25)
$^{74}\text{Rb} \rightarrow ^{74}\text{Kr}$	1.088	1.091	1.071	1.230	1.233	1.258	1.191	1.234	1.63(31)

TABLE II. Excitation energies E_x for the $0^+ \rightarrow 0^+$ superallowed transitions measured by taking the ground state of the corresponding even-even nuclei as reference. In the comparison with the experimental values taken from the recent survey [19], the corrections due to the proton-neutron mass difference in particle-hole configurations are made for the calculated results. All units are in MeV.

	Expt.	PKO1	PKO1*	DD-ME2
$^{10}\text{C} \rightarrow ^{10}\text{B}$	-1.908	-1.698	-2.307	-2.236
$^{14}\text{O} \rightarrow ^{14}\text{N}$	-2.831	-2.420	-2.989	-3.081
$^{18}\text{Ne} \rightarrow ^{18}\text{F}$	-3.402	-3.195	-3.497	-3.451
$^{26}\text{Si} \rightarrow ^{26}\text{Al}$	-4.842	-4.531	-5.139	-5.110
$^{30}\text{S} \rightarrow ^{30}\text{P}$	-5.460	-4.845	-5.326	-5.395
$^{34}\text{Ar} \rightarrow ^{34}\text{Cl}$	-6.063	-5.559	-6.129	-6.278
$^{38}\text{Ca} \rightarrow ^{38}\text{K}$	-6.612	-6.035	-6.611	-6.775
$^{42}\text{Ti} \rightarrow ^{42}\text{Sc}$	-7.000	-6.661	-6.970	-6.964
$^{26}\text{Al} \rightarrow ^{26}\text{Mg}$	4.233	3.908	4.372	4.350
$^{34}\text{Cl} \rightarrow ^{34}\text{S}$	5.492	5.062	5.428	5.561
$^{38}\text{K} \rightarrow ^{38}\text{Ar}$	6.044	5.557	5.936	6.083
$^{42}\text{Sc} \rightarrow ^{42}\text{Ca}$	6.426	6.118	6.333	6.333
$^{54}\text{Co} \rightarrow ^{54}\text{Fe}$	8.244	7.720	8.221	8.240
$^{66}\text{As} \rightarrow ^{66}\text{Ge}$	9.579	9.044	9.488	9.677
$^{70}\text{Br} \rightarrow ^{70}\text{Se}$	9.970	9.632	9.805	9.852
$^{74}\text{Rb} \rightarrow ^{74}\text{Kr}$	10.417	10.005	10.349	10.437

calculations with PKO1 [16], PKO2 [29], PKO3 [29] effective interactions, as well as by self-consistent RH+RPA calculations with DD-ME1 [26], DD-ME2 [30], NL3 [23], TM1 [24] effective interactions. The results obtained by shell model calculations (T&H) [9] are also listed for comparison. The present corrections δ_c range from about 0.1% for the lightest nucleus ^{10}C to about 1.2% for the heaviest nucleus ^{74}Rb , which are 2–3 times smaller than the T&H results. It is noticed that even smaller values of δ_c compared to the shell model calculations have been recently obtained in Ref. [31] using perturbation theory. In addition, in Table II the excitation energies E_x for the $0^+ \rightarrow 0^+$ superallowed transitions corresponding to PKO1 and DD-ME2 are shown as examples. These energies are measured by taking the ground state of the corresponding even-even nuclei as reference. In the comparison with the experimental values taken from the recent survey [19], the corrections due to the proton-neutron mass difference in particle-hole configurations are made for the calculated results. A good agreement between the data and the calculated ones can be seen in Table II.

In Table I, it is found that the present isospin symmetry-breaking corrections δ_c for each nucleus can be unambiguously divided into two categories, those obtained by RHF+RPA calculations and those obtained by RH+RPA calculations. Comparing these two categories, it is seen that the corrections δ_c of RHF+RPA are systematically smaller than those of RH+RPA. On the other hand, it is also found that within one category the corrections δ_c are not sensitive to specific effective interactions or the structure of the Lagrangian density. For instance, within the RH+RPA framework, both the Lagrangian densities with density-dependent meson-nucleon couplings (DD-ME1, DD-ME2) or with nonlinear meson couplings (NL3, TM1) lead to quite similar results.

To understand this systematic discrepancy between RHF+RPA and RH+RPA, it must be kept in mind that in RHF+RPA the exchange (Fock) terms of mesons and photon are kept in both the mean field and RPA levels, whereas they are neglected altogether in RH+RPA. Among all the Fock terms, we expect, in particular, the exchange terms of the Coulomb field to play an important role due to the following reason. The IAS would be degenerate with its isobaric multiplet partners, i.e., $E_x = 0$, and it would contain 100% of the model-independent sum rule (14), i.e., $\delta_c = 0$, if the nuclear Hamiltonian commutes with the isospin raising and lowering operators T_{\pm} . This would be true when the Coulomb field is switched off. While this degeneracy is broken by the mean field approximation, no matter the exchange terms of mesons are included or not, it can be restored by the RPA calculations as long as the RPA calculations are self-consistent [32]. Therefore, the Coulomb field is essential for the $0^+ \rightarrow 0^+$ superallowed transitions and the Coulomb exchange (Fock) term should be responsible for the different isospin symmetry-breaking corrections δ_c in RHF+RPA and RH+RPA approaches.

In order to verify the above argument, we have performed the following calculations. Using PKO1, the Hartree-Fock calculations are performed by switching off the exchange contributions of the Coulomb field. From the single-particle spectra thus obtained, self-consistent RPA calculations are then performed. One may notice that in such calculations some nuclear properties including binding energies and rms radii can no longer be reproduced. However, this does not hinder us from discussing the physics we are concerned with. The isospin symmetry-breaking corrections δ_c and the excitation energies E_x thus obtained are listed in the column denoted as PKO1* in Tables I and II. It is seen that these results are almost the same as those of RH+RPA calculations with DD-ME1, DD-ME2, NL3, and TM1, i.e., by switching off the exchange contributions of the Coulomb field, E_x and δ_c in RHF+RPA calculations recover the results in RH+RPA calculations. In other words, although the meson exchange terms can be somehow effectively included by adjusting the parameters in the direct terms, this has not been done for the Coulomb part in the usual RH approximation.

Therefore, one can conclude that the proper treatments of the Coulomb field is very important to extract the isospin symmetry-breaking corrections δ_c .

B. Nucleus-independent $\mathcal{F}t$ values

Among the $0^+ \rightarrow 0^+$ superallowed transitions listed in Table I, some of their measured ft values are summarized in a recent survey [19]. To obtain the nucleus-independent $\mathcal{F}t$ values from each experimental ft value, apart from the isospin symmetry-breaking corrections δ_c in Table I, one still needs the values of the transition-dependent radiative corrections δ'_R and nuclear-structure-dependent radiative corrections δ_{NS} .

Using the δ'_R and δ_{NS} values from recent calculations [9], δ_c in Table I, and measured ft values [19], the nucleus-independent $\mathcal{F}t$ values for superallowed Fermi β decays are listed in Table III together with the average $\overline{\mathcal{F}t}$ values and the

TABLE III. Nucleus-independent $\mathcal{F}t$ values. The average $\overline{\mathcal{F}t}$ value and the normalized χ^2/ν appear at the bottom. All units are in s.

	PKO1	PKO2	PKO3	PKO1*	DD-ME1	DD-ME2	NL3	TM1
$^{10}\text{C} \rightarrow ^{10}\text{B}$	3079.6(45)	3079.5(45)	3079.4(45)	3077.5(45)	3077.5(45)	3077.5(45)	3078.3(45)	3078.0(45)
$^{14}\text{O} \rightarrow ^{14}\text{N}$	3078.2(31)	3077.5(31)	3078.3(31)	3076.2(31)	3075.8(31)	3075.6(31)	3076.1(31)	3076.8(31)
$^{34}\text{Ar} \rightarrow ^{34}\text{Cl}$	3081.9(84)	3081.5(84)	3082.0(84)	3079.1(84)	3078.8(84)	3078.6(84)	3076.7(83)	3080.3(84)
$^{26}\text{Al} \rightarrow ^{26}\text{Mg}$	3077.7(13)	3077.7(13)	3077.5(13)	3076.0(13)	3075.8(13)	3075.8(13)	3076.6(13)	3076.4(13)
$^{34}\text{Cl} \rightarrow ^{34}\text{S}$	3083.5(16)	3083.3(16)	3083.6(16)	3081.6(16)	3081.4(16)	3081.3(16)	3081.8(16)	3082.5(16)
$^{38}\text{K} \rightarrow ^{38}\text{Ar}$	3084.1(16)	3083.8(16)	3084.2(16)	3082.1(16)	3081.5(16)	3081.3(16)	3082.4(16)	3077.8(16)
$^{42}\text{Sc} \rightarrow ^{42}\text{Ca}$	3082.7(21)	3082.6(21)	3082.6(21)	3080.7(21)	3079.3(21)	3079.1(21)	3081.3(21)	3081.1(21)
$^{54}\text{Co} \rightarrow ^{54}\text{Fe}$	3083.9(27)	3083.9(27)	3083.8(27)	3081.6(27)	3081.5(27)	3081.6(27)	3082.7(27)	3082.4(27)
$^{74}\text{Rb} \rightarrow ^{74}\text{Kr}$	3094.8(87)	3094.7(87)	3095.3(87)	3090.3(87)	3090.2(87)	3089.4(87)	3091.5(87)	3090.2(87)
average	3081.4(7)	3081.3(7)	3081.4(7)	3079.5(7)	3079.1(7)	3079.0(7)	3080.0(7)	3079.1(7)
χ^2/ν	1.1	1.1	1.1	1.0	1.0	1.0	1.0	1.0

values of chi-square per degree of freedom χ^2/ν , in which the uncertainty of δ_c is taken as zero.

It is found that the chi-square per degree of freedom χ^2/ν is $1.0 \sim 1.1$ s for all effective interactions employed. This indicates the constancy of the nucleus-independent $\mathcal{F}t$ values is satisfied, even though not as well as the shell model calculations in Ref. [19]. It is also found that the $\mathcal{F}t$ values of RHF+RPA are about 2 s larger than those of RH+RPA, which are larger than the difference due to the different effective interactions in either RHF or RH approximations.

The results of RHF+RPA with PKO1, RH+RPA with DD-ME2, and NL3 are plotted as a function of the charge Z for the daughter nucleus in Fig. 1 to illustrate the constancy of the nucleus-independent $\mathcal{F}t$ values. The shaded horizontal band gives the standard deviation, which combines the statistical errors and χ^2/ν , around the average $\overline{\mathcal{F}t}$ value.

In order to get a deeper understanding on the treatment of the Coulomb field, the $\mathcal{F}t$ values from RPA calculations using Skyrme Hartree-Fock (SHF) with SGII effective interaction are shown in panel (b) of Fig. 1, in which the isospin symmetry-

breaking corrections δ_c are taken from the Table I in Ref. [10]. It should be emphasized that in these results the exchange contributions to the Coulomb mean field are treated in Slater approximation. Although this model leads to a similar average $\mathcal{F}t$ value, $\overline{\mathcal{F}t} = 3081.1(7)$ s, it is found that the chi-square per degree of freedom $\chi^2/\nu = 1.5$, i.e., the constancy of the $\mathcal{F}t$ values in this SHF framework is not as good as that given by the relativistic calculations. In particular, the $\mathcal{F}t$ value deduced from the nucleus ^{74}Rb is seriously overestimated.

C. CKM matrix

With the nucleus-independent $\mathcal{F}t$ value, the element V_{ud} of the CKM matrix can be calculated by

$$V_{ud}^2 = \frac{K}{2G_F^2(1 + \Delta_R^V)\overline{\mathcal{F}t}}, \quad (15)$$

where $K/(\hbar c)^6 = 8120.2787(11) \times 10^{-10} \text{ GeV}^{-4} \text{ s}$, $G_F/(\hbar c)^3 = 1.16637(1) \times 10^{-5} \text{ GeV}^{-2}$ [7], and $\Delta_R^V = 2.361(38)\%$ [9]. Then in combination with the other two CKM matrix elements $|V_{us}| = 0.2255(19)$ and $|V_{ub}| = 0.00393(36)$ [7], one can test the unitarity of the matrix.

The element V_{ud} as well as the sum of squared top-row elements of the CKM matrix are listed in Table IV. The uncertainties of the present results are underestimated to some extent as the uncertainty of δ_c is assumed to be zero and

TABLE IV. The element V_{ud} and the sum of squared top-row elements of the CKM matrix.

	$ V_{ud} $	$ V_{ud} ^2 + V_{us} ^2 + V_{ub} ^2$
PKO1	0.97273(27)	0.9971(10)
PKO2	0.97275(27)	0.9971(10)
PKO3	0.97273(27)	0.9971(10)
PKO1*	0.97303(26)	0.9977(10)
DD-ME1	0.97309(26)	0.9978(10)
DD-ME2	0.97311(26)	0.9978(10)
NL3	0.97295(26)	0.9975(10)
TM1	0.97309(26)	0.9978(10)

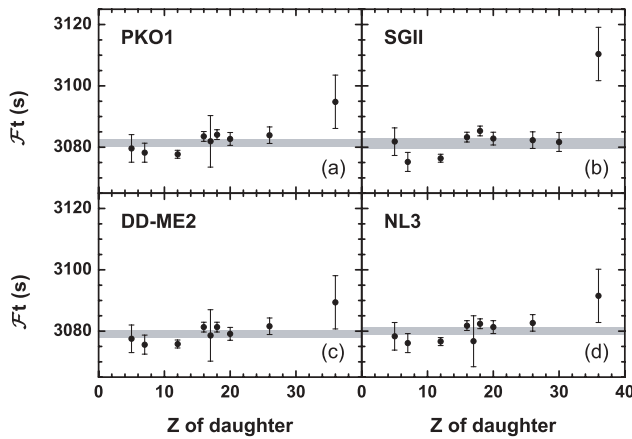


FIG. 1. Nucleus-independent $\mathcal{F}t$ values as a function of the charge Z for the daughter nucleus. The values of δ_c are respectively obtained by RHF+RPA calculations with PKO1 (a), by RH+RPA calculations with DD-ME2 (c), and NL3 (d), as well as by SHF+RPA calculations with SGII [10] (b). The shaded horizontal band gives one standard deviation around the average $\overline{\mathcal{F}t}$ value.

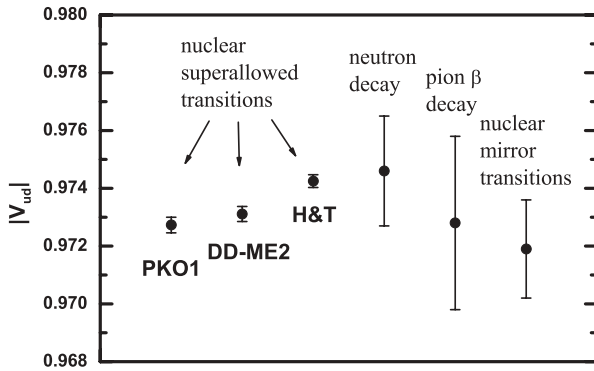


FIG. 2. The element V_{ud} of the CKM matrix obtained by RHF+RPA calculations with PKO1 and by RH+RPA calculations with DD-ME2 in comparison with those in shell model (H&T) [19] as well as in neutron decay [7], pion β decay [5] and nuclear mirror transitions [6].

the systematic errors are not taken into account. In Fig. 2, the element V_{ud} of the CKM matrix obtained by RHF+RPA calculations with PKO1 and by RH+RPA calculations with DD-ME2 are shown in comparison with those in the shell model (H&T) [19] as well as in neutron decay [7], pion β decay [5], and nuclear mirror transitions [6].

It can be clearly seen in Table IV that the matrix element $|V_{ud}|$ determined by the $0^+ \rightarrow 0^+$ superallowed transitions mainly depends on the treatment of the Coulomb field and less sensitive to the particular effective interactions. Switching either on or off the exchange contributions of the Coulomb field, the discrepancy caused by different effective interactions is much smaller than the statistic deviation. It is interesting to note that the present $|V_{ud}|$ values well agree with those obtained in neutron decay, pion β decay and nuclear mirror transitions. However, the sum of squared top-row elements considerably deviates from the unitarity condition, which is in contradiction with the conclusion in shell model calculations (H&T) [19]. This calls for more intensive investigations in the future. For example, mean field and RPA calculations including the proper neutron-proton mass difference, isoscalar and isovector pairing, and deformation should be done. It should also be emphasized that apart from the proper treatment of pairing by either BCS or Bogoliubov approaches, the particle number projection must be implemented as well in order to remove the artificial isospin symmetry breaking effects due to the particle number violation.

IV. SUMMARY AND PERSPECTIVES

In summary, self-consistent relativistic RPA approaches are applied to calculate the isospin symmetry-breaking corrections δ_c for the $0^+ \rightarrow 0^+$ superallowed transitions. In the RHF+RPA framework the density-dependent effective interactions PKO1, PKO2, and PKO3 are employed, while in the RH+RPA framework the density-dependent effective interactions DD-ME1 and DD-ME2 as well as the nonlinear effective interactions NL3 and TM1 are used.

It is found that the proper treatments of the Coulomb field is very important to extract the isospin symmetry-breaking corrections δ_c . By switching off the exchange contributions of the Coulomb field, E_x and δ_c in RHF+RPA calculations recover the results in RH+RPA calculations. In other words, although the meson exchange terms can be somehow effectively included by adjusting the parameters in the direct terms, this has not been done for the Coulomb part in the usual RH approximation.

With the isospin symmetry-breaking corrections δ_c calculated by relativistic RPA approaches, the nucleus-independent $\mathcal{F}t$ values are obtained in combination with the experimental ft values in the most recent survey and the improved radiative corrections. It is found that the constancy of the $\mathcal{F}t$ values is satisfied for all self-consistent relativistic RPA calculations here. It is also found that the $\mathcal{F}t$ values of RHF+RPA are about 2 s larger than those of RH+RPA, which are larger than the difference due to the different effective interactions in either RHF or RH approximations.

The values of $|V_{ud}|$ thus obtained well agree with those obtained in neutron decay, pion β decay, and nuclear mirror transitions. However, the sum of squared top-row elements considerably deviates from the unitarity condition, which is in contradiction with the conclusion in shell model calculations (H&T) [19].

For the further studies, more intensive investigations including the proper neutron-proton mass difference, isoscalar and isovector pairing, and deformation should be done.

ACKNOWLEDGMENTS

This work is partly supported by Major State 973 Program 2007CB815000, the NSFC under Grant Nos. 10435010, 10775004, and 10221003. One of the authors (H.L.) is grateful to the French Embassy in Beijing for the financial support for his stay in France.

- [1] N. Cabibbo, Phys. Rev. Lett. **10**, 531 (1963).
- [2] M. Kobayashi and T. Maskawa, Prog. Theor. Phys. **49**, 652 (1973).
- [3] J. C. Hardy and I. S. Towner, Phys. Rev. C **71**, 055501 (2005).
- [4] D. Thompson, J. Phys. G **16**, 1423 (1990).
- [5] D. Počanić *et al.*, Phys. Rev. Lett. **93**, 181803 (2004).
- [6] O. Naviliat-Cuncic and N. Severijns, Phys. Rev. Lett. **102**, 142302 (2009).
- [7] C. Amsler *et al.*, Phys. Lett. **B667**, 1 (2008).
- [8] W. J. Marciano and A. Sirlin, Phys. Rev. Lett. **96**, 032002 (2006).

- [9] I. S. Towner and J. C. Hardy, Phys. Rev. C **77**, 025501 (2008).
- [10] H. Sagawa, N. Van Giai, and T. Suzuki, Phys. Rev. C **53**, 2163 (1996).
- [11] J. Engel, M. Bender, J. Dobaczewski, W. Nazarewicz, and R. Surman, Phys. Rev. C **60**, 014302 (1999).
- [12] S. Fracasso and G. Colò, Phys. Rev. C **72**, 064310 (2005).
- [13] C. De Conti, A. P. Galeao, and F. Krmpotić, Phys. Lett. **B444**, 14 (1998).
- [14] N. Paar, T. Nikšić, D. Vretenar, and P. Ring, Phys. Rev. C **69**, 054303 (2004).

- [15] H. Liang, N. Van Giai, and J. Meng, Phys. Rev. Lett. **101**, 122502 (2008).
- [16] W. H. Long, N. Van Giai, and J. Meng, Phys. Lett. **B640**, 150 (2006).
- [17] W. H. Long, H. Sagawa, J. Meng, and N. Van Giai, Phys. Lett. **B639**, 242 (2006).
- [18] B. Y. Sun, W. H. Long, J. Meng, and U. Lombardo, Phys. Rev. C **78**, 065805 (2008).
- [19] J. C. Hardy and I. S. Towner (2008), arXiv:0812.1202 [nucl-ex].
- [20] B. D. Serot and J. D. Walecka, *Advances in Nuclear Physics Vol. 16: The Relativistic Nuclear Many Body Problem* (Plenum Press, New York, 1986).
- [21] A. Bouyssy, J.-F. Mathiot, N. Van Giai, and S. Marcos, Phys. Rev. C **36**, 380 (1987).
- [22] J. Meng, H. Toki, S. G. Zhou, S. Q. Zhang, W. H. Long, and L. S. Geng, Prog. Part. Nucl. Phys. **57**, 470 (2006).
- [23] G. A. Lalazissis, J. König, and P. Ring, Phys. Rev. C **55**, 540 (1997).
- [24] Y. Sugahara and H. Toki, Nucl. Phys. **A579**, 557 (1994).
- [25] W. Long, J. Meng, N. Van Giai, and S.-G. Zhou, Phys. Rev. C **69**, 034319 (2004).
- [26] T. Nikšić, D. Vretenar, P. Finelli, and P. Ring, Phys. Rev. C **66**, 024306 (2002).
- [27] T. Nikšić, D. Vretenar, and P. Ring, Phys. Rev. C **66**, 064302 (2002).
- [28] J. Meng, Nucl. Phys. **A635**, 3 (1998).
- [29] W. H. Long, H. Sagawa, J. Meng, and N. Van Giai, Europhys. Lett. **82**, 12001 (2008).
- [30] G. A. Lalazissis, T. Nikšić, D. Vretenar, and P. Ring, Phys. Rev. C **71**, 024312 (2005).
- [31] N. Auerbach, Phys. Rev. C **79**, 035502 (2009).
- [32] C. A. Engelbrecht and R. H. Lemmer, Phys. Rev. Lett. **24**, 607 (1970).